

1 **Age and strain related aberrant  $\text{Ca}^{2+}$  release is associated with sudden cardiac death in the**  
2 **ACTC E99K mouse model of hypertrophic cardiomyopathy**

3

4 Abbreviated title:  $\text{Ca}^{2+}$  regulation in E99K mouse heart

5

6 Christina T Rowlands, Thomas Owen, Saheed Lawal, Shuangyi Cao, Samata S Pandey, Hsiang-  
7 Yu Yang, Weihua Song, Ross Wilkinson, Anita Alvarez-Laviada, Katja Gehmlich, Steven B  
8 Marston, Kenneth T MacLeod.

9

10

11 National Heart & Lung Institute,  
12 Imperial Centre for Translational and Experimental Medicine  
13 Imperial College  
14 Hammersmith Hospital  
15 Du Cane Road  
16 London W12 0NN

17

18 Correspondence to Kenneth T MacLeod at the above address

19 Tel: +44 (0)20 7594 2734

20 email: k.t.macleod@imperial.ac.uk

21

22

23 Contributions of the authors

24 CR, TO, SL SC, SP, H-SY, WS, RW AA-L performed the experiments, analysed the data,  
25 constructed figures and contributed to writing the manuscript

26 KG bred the transgenic mice on the C57Bl6 background and contributed to writing the manuscript

27 SM and KM conceived the project, obtained funding, directed the project, assisted with data

28 analyses and wrote the manuscript

29

30

31

32

## **Abstract, Key Words, New and Noteworthy**

Patients with hypertrophic cardiomyopathy (HCM), particularly young adults, can die from arrhythmia but the mechanism underlying abnormal rhythm formation remains unknown. C57Bl6 x CBA/Ca mice carrying a cardiac actin (*ACTC*) E99K (Glu99Lys) mutation reproduce many aspects of human HCM including increased myofilament  $\text{Ca}^{2+}$  sensitivity and sudden death in a proportion (up to 40%) of young (28-40 day old) animals. We studied the hearts of transgenic (TG – *ACTC* E99K) mice and their non-transgenic (NTG) littermates when they were in their vulnerable period (28-40 days old) and when they were adult (8-12 weeks old). Ventricular myocytes were isolated from the hearts of TG and NTG mice at these two time points. We also examined the hearts of mice that died suddenly (SCD). SCD animals had approximately four times more collagen compared with age-matched NTG mice yet myocyte cell size was normal. Young TG mice had double the collagen content of NTG mice. Contraction and  $\text{Ca}^{2+}$  transients were greater in cells from young TG mice compared with their NTG littermates but not in cells from adult mice (TG or NTG). Cells from young TG mice had greater propensity for  $\text{Ca}^{2+}$  waves than NTG littermates and, despite similar SR  $\text{Ca}^{2+}$  content, a proportion of these cells had larger  $\text{Ca}^{2+}$  spark mass. We found that the probability of SCD in young TG mice is increased when the mutation is expressed in animals with a CBA/Ca background and almost eliminated in mice bred on a C57Bl6 background. The latter TG mice had normal cellular  $\text{Ca}^{2+}$  homeostasis.

### **Key words**

$\text{Ca}^{2+}$  sparks,  $\text{Ca}^{2+}$  waves, sarcoplasmic reticulum, myofilament sensitivity

### **New and Noteworthy**

- Mice with the ACTCE99K HCM mutation are prone to sudden cardiac death around 40 days, associated with increased  $\text{Ca}^{2+}$ -transients, spark mass and fibrosis
- However, adult survivors have normal  $\text{Ca}^{2+}$ -transients and spark density accompanied by hypertrophy
- Penetrance of the sudden cardiac death phenotype depends on the genetic background of the mouse.

## 73 Introduction

74 Inherited heart diseases are responsible for a significant proportion of cardiac-related death and  
75 morbidity and are currently difficult to treat. Hypertrophic cardiomyopathy (HCM) is a primary  
76 disease of cardiac muscle clinically defined by a hypertrophied, non-dilated left ventricle in the  
77 absence of any other aetiology. It is a common disorder affecting 1 in 500 of the population and is  
78 the leading cause of sudden cardiac death in young individuals(27). HCM is largely caused by  
79 monogenic mutations in genes encoding sarcomeric proteins, commonly *MYH7* and *MYBPC3*,  
80 though about 12% are in genes encoding proteins of the thin filament(1). HCM presents with a  
81 variable sequence of clinical events. Some patients can remain stable over long periods of time  
82 while others suffer adverse events including sudden cardiac death (SCD), embolic stroke and heart  
83 failure. Sudden death (not associated with heart failure) is the most devastating of the adverse  
84 events and most frequently occurs in adolescents and young adults though it can also extend into  
85 later life(28).

86  
87 The molecular basis of HCM has been extensively studied and the most likely primary mechanism  
88 involves derangement of  $\text{Ca}^{2+}$  regulation of the sarcomere(30). A recent literature search yielded  
89 71 independent measurements of increased  $\text{Ca}^{2+}$ -sensitivity due to HCM mutations, ranging from a  
90 1.15 to a 3.8-fold increase (mean  $1.87 \pm 0.07$ )(29). Thus the cardiac muscle in patients with HCM  
91 has a hypercontractile phenotype that causes incomplete relaxation and diastolic dysfunction.  
92 Moreover, the increased  $\text{Ca}^{2+}$ -sensitivity has been proposed to predispose the heart to certain  
93 forms of arrhythmia that may provoke sudden cardiac death(18; 46; 47).

94  
95 We have developed a transgenic (TG) mouse with a cardiac actin mutation *ACTC* E99K  
96 (Glu99Lys)(34) that enables us to investigate the proposed mechanism of sudden cardiac death.  
97 The TG mice express the mutation in 50% of the total sarcomeric actin. This level is achieved by  
98 21 days and is maintained throughout life. The mutation causes an increase in myofilament  $\text{Ca}^{2+}$ -  
99 sensitivity observed in single myofilaments using *in vitro* motility assays, myofibrils and isolated  
100 papillary muscle(46; 47). Not only do these mice reproduce the apical hypertrophy, myocyte  
101 disarray, interstitial fibrosis, arrhythmias and the subsequent development of heart failure noted in  
102 human HCM, but also they have a striking predisposition to SCD between 4 and 6 weeks of age,  
103 which is more pronounced in females(46; 47). Up to 40% of the mice died during this early  
104 vulnerable period whilst survivors had a normal life-span despite less efficient cardiac work and in  
105 later life experiencing progressive cardiac hypertrophy, fibrosis and diastolic dysfunction. The close  
106 recapitulation of the human condition by this mouse model offers an opportunity to investigate the  
107 mechanism underlying SCD and account for the observation that only a proportion of mice dying  
108 early in life. The underlying cause of the SCD in patients with HCM is usually arrhythmia and  
109 Baudenbacher et al.(3) demonstrated that  $\text{Ca}^{2+}$  sensitization *per se* can be pro-arrhythmic in the  
110 absence of typical anatomical abnormalities produced by HCM. The mechanism underlying

111 arrhythmia generation when the primary disturbance in the cell biology is a sarcomeric mutation  
112 remains unknown.  
113  
114 We have studied the hearts of TG mice and their non-transgenic (NTG) littermates when they are  
115 in their vulnerable period (28-40 days old), when they are adult (8-12 weeks old) and also  
116 examined mice that died suddenly. We have investigated if the development of hypertrophy and  
117 fibrosis correlates with SCD and if the higher  $\text{Ca}^{2+}$  sensitivity in TG mice disturbs intracellular  $\text{Ca}^{2+}$   
118 homeostasis causing changes to cellular  $\text{Ca}^{2+}$  handling and electrophysiological stability. We show  
119 that the underlying pro-arrhythmic mechanism is that some young TG mice have an increased  
120 propensity for spontaneous  $\text{Ca}^{2+}$  release that could lead to the formation of afterdepolarisations so  
121 predisposing their hearts to potentially fatal arrhythmias. Moreover, we find that the probability that  
122 young TG mice have this aberrant cellular  $\text{Ca}^{2+}$  homeostasis is dependent on the background  
123 strain of the mice.  
124

## 125 **Methods**

126

### 127 *ACTC E99K mice*

128 The generation of ACTC E99K transgenic mice is described by Song et al(46). Male ACTC E99K  
129 mice were bred with female C57Bl6 x CBA/Ca F1 hybrid mice and the resulting phenotype is  
130 described in detail by Song et al(46). Mice were housed at  $21 \pm 1^\circ\text{C}$  on a 12h light : dark cycle and  
131 provided with standard feed and water *ad libitum*. All procedures on the mice were performed in  
132 accordance with the United Kingdom Animals (Scientific Procedures) Act of 1986, EU Directive  
133 2010/63/EU for animal experiments and with University ethical approval. To obtain heart tissue,  
134 mice were deeply anaesthetised using 5% isoflurane in 100% oxygen and subsequently killed by  
135 cervical dislocation. Tissues were then removed from the animal.

136

### 137 *Genotyping transgenic mice*

138 Ear notch samples produced approximately 5µg DNA. DNA extraction was performed using a  
139 Qiagen DNeasy blood & tissue kit (Qiagen, UK) according to the manufacturer's instructions and  
140 the extracted DNA was stored at  $4^\circ\text{C}$  until required for PCR. PCR primers were obtained from  
141 Invitrogen (UK). The forward primer is located in the promoter element of the transgene (MHC-F  
142 sequence (5'-3') TGACAGACAGATCCCTCCTATCTCC and the reverse primer is located in the  
143 mutant actin (ACTC-R) (5'-3') GGCATCTTAGAAGCATTGCGG.

144

### 145 *RNA extraction and gene expression analysis*

146 Heart tissue (20 mg) was homogenized and lysed in 350 µl TRI Reagent buffer (Sigma). Primers  
147 used for gene expression analysis are listed below. RNA was extracted with RNeasy Mini Kit  
148 (Qiagen). NanoDrop 2000 (ThermoScientific) was used for quantification of the RNA. Reverse  
149 Transcription Polymerase Chain Reaction (RT-PCR) was performed with the High Capacity cDNA  
150 Reverse Transcription Kit (Applied Biosystems) based on the manufacturer instructions. Real-time  
151 PCR were performed with TaqMan gene expression assays (Applied Biosystems). All samples  
152 were run in triplicate with the housekeeping gene, GAPDH. qPCR data was analysed by the  
153 comparative Ct method ( $2^{-[\Delta\Delta\text{Ct}]}$  method) using the average of three technical replicates.

154

### 155 *Western blotting analysis*

156 Heart tissues were manually homogenized in T-PER Tissue Protein Extraction Reagent (Thermo  
157 Scientific) containing 2 µg/mL each of the protease inhibitors chymostatin, leupeptin and pepstatin  
158 A. Six times of the volume of the T-PER solution to the weight of frozen heart tissue was added to  
159 dissolve the pulverised tissue. The same amount of 2x SDS buffer was added (20 mM Tris-HCl, 5  
160 % SDS, 10 %  $\beta$ - mercaptoethanol). The proteins were transferred onto a 0.2 µm nitrocellulose  
161 membrane using the TransBlot Turbo Transfer System (BioRad). Proteins were visualised using  
162 Pierce Reversible Protein Stain Kit (ThermoScientific) and imaged using G:Box Chemi XT Imager

(Syngene). The membranes were blocked with 20 % SeaBlock blocking buffer (Pierce Chemical), 0.1 % Tween 20 in phosphate-buffered saline (PBS, pH 7.2- 7.4) for 1 hour. The custom-made rabbit polyclonal antibody specific to the E99K mutation was diluted at 5000:1 in 20 % blocking solution and incubated at 4 °C overnight with agitation. The membranes were washed with PBS containing 0.1 % Tween 20 three times for 5 minutes each, followed incubation with the secondary antibody for 1 hour at room temperature with agitation. Three times wash steps in PBS were repeated. Immunoreactivity bands were visualised using Amersham ECL Select Western Blotting Detection Reagents (GE Healthcare) and detected in the imager. GeneTools (Syngene) was used for the quantification of the band density. The density of antibody relative to the density of  $\alpha$ -actinin on protein stained membrane was used to control for loading variation between samples.

#### *Histology and immunohistochemistry*

Freshly dissected hearts were stored in liquid nitrogen. They were gradually thawed and then fixed in 4 % paraformaldehyde (PFA) overnight at 4°C and cryo-protected with 30 % sucrose. The fixed hearts were frozen in optimum cutting temperature (OCT) compound vertically, and transverse cryosections were cut at 7  $\mu$ m intervals.

##### 1) Wheat germ agglutinin (WGA) staining for cell size

For WGA staining, sections were rehydrated with PBS. Slides were blocked with 20 % goat serum diluted in PBS for 30 minutes at room temperature (RT). Then, slides were incubated with Alexa Fluor<sup>®</sup> 488 conjugate of WGA (10  $\mu$ g/ml, diluted in PBS, Invitrogen) for 30 minutes with protection from the light. Slides were washed twice with PBS, mounted in Vectashield with DAPI (Vector Labs), and covered with coverslips. Images were recorded with fluorescence microscopy (Zeiss Axio Observer Inverted Widefield Microscope with LED illumination) at excitation and emission of 495 nm and 519 nm, respectively. For each section, 4 images were captured using 20x magnification and in each image 50-60 cells were calculated in ImageJ software.

##### 2) Picro-sirius red (PSR) staining for collagen

The sections were rehydrated with distilled water and stained in a solution of 0.1% Sirius red F3BA in saturated aqueous picric acid (Sigma-Aldrich) for 35 min at room temperature (RT), followed by 4 washing steps in 100 % methanol, as modified from other studies (24). Subsequently, the slides were rinsed twice in xylene, for 10 min each. Slides were mounted with Vectashield with DAPI (Vector Labs), covered with coverslips and left to dry overnight at RT. A series of images of one section were acquired at 10x magnification and were automatically stitched together using bright field mode of the LSM-780 inverted confocal laser scanning microscope (Zeiss). Collagen content was quantified in ImageJ software. Total collagen content was defined as the proportion of positive pixels to total pixels of stained area.

201 *Isolation of cardiac myocytes and loading with  $\text{Ca}^{2+}$ -sensitive dyes*

202 Cardiac myocytes were isolated by enzymatic digestion and loaded with  $\text{Ca}^{2+}$ -sensitive dyes using  
203 established techniques(24; 25; 45; 50).

204

205  *$\text{Ca}^{2+}$  transients and cell length measurements*

206 Fura-2 was excited at 360 and 380 nm and fluorescence collected at 510 nm using an Ionoptix  
207 system (Ionoptix, Milton, MA) with a PMT connected to a PC running IonWizard software. Cell  
208 contraction was measured using a CCD video camera (MyoCam-S, IonOptix corp. Milton, MA,  
209 USA) also connected to the PC running IonWizard software.

210

211  *$\text{Ca}^{2+}$  sparks and waves*

212  $\text{Ca}^{2+}$  sparks were recorded by previously described methods and analysis of the line scan images  
213 was performed using ImageJ (NIH, USA) with the SparkMaster plugin(40) and custom macros(45).  
214 Detection criteria for  $\text{Ca}^{2+}$  sparks were set at 3.8 times the standard deviation above the mean  
215 background value. Spark mass was calculated using the formulae derived by Hollingworth et  
216 al(16). To assess wave frequency and characteristics, cells were stimulated at up to 5 Hz for 30s.  
217 Field stimulation was then stopped and waves were recorded during a subsequent 20s period.

218

219 *Determination of SR Ca content*

220 Determinations of SR Ca content were made using the change in fura-2 ratio as a qualitative index  
221 of load following rapid application of 10 mM caffeine in  $\text{Na}^+$ -free /  $\text{Ca}^{2+}$ -free solution. The caffeine  
222 evokes SR Ca release while the zero  $\text{Na}^+$  / zero  $\text{Ca}^{2+}$  solution prevents  $\text{Na}^+/\text{Ca}^{2+}$  exchange from  
223 effluxing  $\text{Ca}^{2+}$  and attenuating the size of the induced transient. Assessments of  $\text{Na}^+/\text{Ca}^{2+}$   
224 exchange and SR  $\text{Ca}^{2+}$  ATPase function were made by comparing the decay times of the caffeine-  
225 induced  $\text{Ca}^{2+}$  transients either in the continued presence of caffeine alone (for  $\text{Na}^+/\text{Ca}^{2+}$  exchange  
226 function) or in  $\text{Na}^+$ -free /  $\text{Ca}^{2+}$ -free solution following caffeine removal (for SR  $\text{Ca}^{2+}$  ATPase  
227 function), (see Figure 4)(2).

228

229 *Statistical analyses*

230 Data are presented as mean  $\pm$  SEM and statistical significance between means was taken when  $P$   
231  $< 0.05$ . Data sets were normally distributed except for Ca spark parameters. Logarithmic  
232 transformations of these data were carried out before the Student t test or ANOVA was applied.

233

234

## Results

### *Timeline for development of HCM phenotype*

Using an antibody specific to the *ACTC* E99K mutation we found that expression of the mutation is switched on shortly after birth and reaches adult levels between P14 and P21, well before the SCD window. Post-mortem analysis of SCD mice showed *ACTC* E99K expression levels the same as transgenic adult survivors (Figure 1).

We measured ventricular muscle cell sizes in two ways. Cross sections of ventricular wall were stained with wheatgerm agglutinin (WGA) and cell cross sectional area was measured using planimetry. Figure 2 panels A - C show representative histological sections of hearts from (A) NTG, (B) *ACTC* E99K TG mice and (C) *ACTC* E99K TG mice that suffered sudden cardiac death. WGA sections are shown at the right of each panel. Cell areas of young TG mice and TG mice that died suddenly were not significantly different from NTG mice (Figure 2D). Cell hypertrophy was observed in older TG mice but in NTG hearts, cell areas were the same in young and adult mice. Cell areas and perimeter lengths of enzymatically-dissociated ventricular myocytes were measured following image capture and analysis by ImageJ. Young TG mice had smaller perimeters than their NTG counterparts ( $173 \pm 3$  vs  $297 \pm 4$   $\mu\text{m}$ ,  $p < 0.001$ ) and reduced cell areas ( $1711 \pm 44 \mu\text{m}^2$  vs  $2201 \pm 66 \mu\text{m}^2$ ,  $p < 0.001$ ; (178 cells from 15 NTG animals, 125 cells from 10 TG animals). These combined approaches of cell size measurement indicate that cell hypertrophy does not contribute to the SCD phenotype.

Figure 2 panels A - C also show representative histological sections of hearts stained with picrosirius red for collagen determination. These are shown in the left-hand side of each panel. We found a strong association between the extent of cardiac fibrosis and SCD in TG mice. These data (Figure 2E) suggest there is approximately four times more collagen in SCD mice compared with age-matched NTG mice. Young TG mice have approximately double the collagen content of NTG mice and notably, NTG and TG mice bred on pure C57Bl6 backgrounds have similar collagen content to the NTG hybrid mice. These findings were supported by measurements of *COL1A1* and *COL3A1* gene expression (Figure 2F and G).

### *Contraction and $\text{Ca}^{2+}$ transients*

Figure 3 shows that ventricular myocytes isolated from young transgenic mice (TG) (between 20 and 45 days old) have a hypercontractile phenotype (panel A) and larger  $\text{Ca}^{2+}$  transients (panel B) compared with their NTG littermates and with adult mice of both genotypes (panels B and D). The larger contractions can be explained by higher myofilament  $\text{Ca}^{2+}$  sensitivity in TG mice found in previous work(46; 47). The larger contractions in young TG animals are observed over a range of stimulation frequencies. In contrast, ventricular myocytes isolated from adult *ACTC* E99K mice (between 56 and 84 days old) do not have a hypercontractile phenotype and have smaller  $\text{Ca}^{2+}$



transients compared with their NTG littermates (Figure 3 B and D). The  $\text{Ca}^{2+}$  transient amplitudes recorded from TG cardiac myocytes isolated from the younger animals had a larger spread of data points extending above the range seen in the control NTG group (panel E). Almost a quarter of the young TG cells exhibited  $\text{Ca}^{2+}$  transients above the largest Fura-2 ratio observed in young NTG cells ( $\sim 0.9 \Delta\text{Fura-2}$  ratio, dashed lines on panel E). In contrast, in the adult group of mice (8-12 weeks) the  $\text{Ca}^{2+}$  transient amplitude range was not significantly different between NTG and TG cells (panel F). Mean  $\text{Ca}^{2+}$  transient amplitudes recorded in myocytes isolated from adult and young NTG hearts were not different. TG animals (both young and adult) had lower diastolic Fura-2 ratios (Table 1) but there was no difference in decay times of the caffeine-induced  $\text{Ca}^{2+}$  transients between NTG or TG cells either in the continued presence of caffeine or in  $\text{Na}^+$ -free /  $\text{Ca}^{2+}$ -free solution suggesting unchanged  $\text{Na}^+/\text{Ca}^{2+}$  exchange and SR  $\text{Ca}^{2+}$  ATPase functions.

284

#### 285 $\text{Ca}^{2+}$ waves

The next experiments were designed to assess if young TG animals exhibited more spontaneous contractions. Cells were paced at 0.5-5.0 Hz for 1 min to load the SR. The stimulation train was followed by a 30 s pause during which spontaneous contractions were recorded (Figure 4A). Figure 4B shows that after stimulation at 1.0 Hz, the frequency of spontaneous contractions is greater in young TG cells compared with their NTG counterparts. Similar relationships were found with  $\text{Ca}^{2+}$  waves measured using Fura-2 (Figure 4C). TG cells showed more spontaneous  $\text{Ca}^{2+}$  wave events compared with cells isolated from NTG littermates – a relationship that remained at all SR loading stimulation frequencies (Figure 4D).

294

The time to the first spontaneous contraction (SC) was measured as the time from the last electrically-stimulated contraction (at 1Hz) to the first SC. This was represented in Kaplan-Meier survival curves as shown in Figure 5. The SC-free survival period was reduced in TG cells ( $p < 0.001$ , Log-Rank curve comparison test). This relationship remained at all stimulation frequencies.

300

The increased occurrence of waves could be a result of an increase in SR  $\text{Ca}^{2+}$  content(8; 42) so we assessed this using rapid application of 10 mM caffeine in a  $\text{Na}^+$ -free /  $\text{Ca}^{2+}$ -free solution. The caffeine evokes SR  $\text{Ca}^{2+}$  release while the  $\text{Na}^+$ -free /  $\text{Ca}^{2+}$ -free solution prevents the  $\text{Na}^+/\text{Ca}^{2+}$  exchange from effluxing  $\text{Ca}^{2+}$  and reducing the size of the induced transient (Figure 6A). The SR  $\text{Ca}^{2+}$  contents of myocytes isolated from young TG mice are not different from their NTG counterparts (Figure 6B) suggesting the increased occurrence of waves in these mice is dependent on some other factor. The SR  $\text{Ca}^{2+}$  contents of myocytes isolated from the adult, surviving TG mice are less than their NTG counterparts (Figure 6C). Since  $\text{Ca}^{2+}$  release depends on SR  $\text{Ca}^{2+}$  content, the reduction in transient size observed in the adult, surviving mice may be explained by a reduction in stored  $\text{Ca}^{2+}$ .

311 *Ca<sup>2+</sup> regulation in male and female TG mice*

312 In previous work we reported that the prevalence of SCD in young ACTC E99K mice is more  
313 frequent in females than males (40% of females vs 25% males die when they are 30-45 days old).  
314 Sex differences in the onset and progression of cardiovascular disease have been noted (31; 37;  
315 39) as well as some variations in cardiomyocyte intracellular Ca<sup>2+</sup> regulation (11; 54). We  
316 examined if there were any alterations in intracellular Ca<sup>2+</sup> regulation between cardiomyocytes  
317 isolated from surviving female and male ACTC E99K mice. We found two significant differences  
318 and these are shown in Figure 7. Although there were no differences in Ca<sup>2+</sup> transient decay times  
319 between the pooled TG and NTG data, the decay of the electrically-stimulated Ca<sup>2+</sup> transient in  
320 female TG myocytes was slower than the transient decay in the male myocytes. Separation of the  
321 data into male and female groups also revealed that the decay times of caffeine-induced Ca<sup>2+</sup>  
322 transients (in the continued presence of caffeine so allowing assessment of Ca<sup>2+</sup> efflux mediated  
323 by the Na<sup>+</sup>/Ca<sup>2+</sup> exchange and slow systems) were slower in TG female myocytes compared with  
324 cells from their NTG littermates. A similar difference was not evident in male myocytes.

325

326 *Ca<sup>2+</sup> sparks*

327 Cells from TG animals (both young and adult) had greater spark frequencies compared with cells  
328 from NTG animals (Figures 8B, C, F and G). However, spark amplitudes were greater in young  
329 TG animals compared with NTG littermates (Figure 8D and E). Spark amplitudes measured in TG  
330 and NTG cells from the older surviving mice were not different (Figure 8H and I). These data were  
331 skewed so log-transformations were used to produce approximately Gaussian distributions  
332 (Figures 8C, E, G and I) and a t-test with Welch's correction was applied.

333

334 Spark mass (an index of the volume integral of the change in Fluo-4 fluorescence and calculated  
335 using the formula derived by Hollingworth et al.(16) was greater in young TG animals compared  
336 with NTG littermates (Figure 9A and B). Figure 9A indicates that the range of spark mass is also  
337 much larger in young TG cells. Again, these data were skewed so log-transformations were used  
338 to produce approximately Gaussian distributions (Figure 9B). An ANOVA with Bonferroni  
339 correction indicated highly significant differences (P < 0.001) between the two groups. The dashed  
340 line in Figure 9A indicates the largest spark mass in the young NTG population for ease of  
341 comparison. Notably, spark masses measured in cells isolated from the older, surviving TG mice  
342 were not different from NTG littermates (Figure 9C and D). Only one spark measured from the TG  
343 group had a mass greater than the largest mass measured in the young NTG group as indicated  
344 by the dashed red line (Figure 9C).

345

346 *The effect of the ACTC E99K mutation depends on strain of mouse.*

347 It is evident that some of the young ACTC E99K mice are phenotypically hypercontractile and have  
348 increased Ca<sup>2+</sup> transients and spark mass whilst the TG survivors are not different from their NTG

349 littermates. Since we are studying the *ACTC* E99K mutation on a hybrid background (C57/Bl6 x  
350 CBA/Ca) a simple explanation would be that mice segregate into two populations – some with  
351 more C57/Bl6 characteristic and some with more CBA/Ca characteristics. To test this idea we  
352 bred our TG mice onto a pure C57Bl6 backgrounds. *ACTC* E99K mice back-crossed with pure  
353 C57/Bl6 females for at least 8 generations, lost the SCD trait (see Figure 10) and young *ACTC*  
354 E99K mice on this pure C57Bl6 background showed low spark masses comparable with NTG  
355 littermates (Figure 9E and F).  
356  
357 When we bred our hybrid *ACTC* E99K males with CBA/Ca females, the first generation showed the  
358 transgenic mice had a greater probability of SCD (Figure 10) but, unfortunately a second back-  
359 crossing yielded no transgenic pups. Kaplan-Meier survival plots of each of these mouse lines are  
360 shown in Figure 10. TG mice bred on a pure C57Bl6 background lose the sharp SCD time window  
361 while the first generation TG mice bred on a CBA/Ca background showed the lowest survival  
362 duration. The hybrid TG mice (on the C57/Bl6 x CBA/Ca background) have an intermediate  
363 survival duration with the now well-described window of SCD around 40 days.

## 364 Discussion

365 Hypertrophic cardiomyopathy is the most common monogenic cardiovascular disease and carries  
366 a significant risk of SCD due to arrhythmias. Adult *ACTC* E99K transgenic mice express the  
367 mutation at 50% of total sarcomeric actin and reproduce many aspects of HCM observed in  
368 humans with this mutation(34; 46) such as apical and septal hypertrophy, trabeculation, myocyte  
369 disarray and interstitial fibrosis.

370 The most striking characteristic of the *ACTC* E99K TG mouse population is the high probability of  
371 SCD in a proportion of young mice. 40% of female and 25% of male mice were reported to die  
372 when they are 30-45 days old(47). In order to understand this we have investigated the changes  
373 that take place in young mice near the vulnerable window (25-40 days) and compared these with  
374 the mice that died suddenly and the adult survivors. The results show that young TG mice have a  
375 different  $\text{Ca}^{2+}$ -regulatory phenotype from the adult TG survivors and that this is strongly dependent  
376 on the genetic background of the mice studied. There are reports of developmental changes in  
377 intracellular  $\text{Ca}^{2+}$  regulation, transverse tubule organisation and EC coupling particularly in the  
378 rat(4; 10; 43; 49) just after birth. However, such changes are an unlikely explanation for the  
379 current findings because the integrity of the transverse tubules systems, synchronization of  
380 triggered  $\text{Ca}^{2+}$  release and EC coupling mechanisms are fully developed by day 20 in mice(41).

381 In common with most sarcomeric mutations that cause HCM, the primary effect of the *ACTC* E99K  
382 mutation is enhanced myofilament  $\text{Ca}^{2+}$  sensitivity and an uncoupling of the relationship between  
383  $\text{Ca}^{2+}$ -sensitivity and troponin I phosphorylation by PKA. Thus the mutation leads to a  
384 hypercontractile phenotype(47). The mechanisms by which this leads to hypertrophy and to  
385 fibrosis are not clear, but Baudenbacher et al. have demonstrated that increased  $\text{Ca}^{2+}$ -sensitivity  
386 *per se* was sufficient to increase the probability of arrhythmia(3). The major secondary  
387 characteristics of HCM seen in patients are hypertrophy and interstitial fibrosis. We could not find  
388 evidence for cellular hypertrophy particularly in the young mice and so the former could not  
389 contribute to the sudden cardiac death phenotype that we observe. On the other hand, young  
390 *ACTC* E99K mice that had died suddenly showed a high level of interstitial fibrosis similar to that  
391 found in other mouse models with SCD at this age(21). Although interstitial fibrosis is unlikely to  
392 be an initiating cause of the events leading up to SCD – since potentially fatal arrhythmias can be  
393 induced by acute  $\text{Ca}^{2+}$ -sensitisation in the absence of fibrosis(3) – it is recognised that fibrosis is  
394 associated with persistent atrial fibrillation, increased anisotropy in ventricular tissue and the  
395 separation of muscle bundles and so provides a substrate for multiple re-entrant circuits perhaps  
396 allowing spontaneous depolarisations to proliferate. This is supported by examination of the hearts  
397 from mice with the *ACTC* E99K transgene that have been bred on a pure C57Bl6 background  
398 which have low levels of fibrosis (38). We note that there are 15% fewer myocytes/square mm in  
399 SCD mice compared with wild-type, suggesting cell death and replacement fibrosis is associated  
400 with the processes leading to SCD.

401  
402 There may also be interaction between fibrosis and  $\text{Ca}^{2+}$  sensitivity and fibrosis and cell-cell  
403 coupling which may create a potentially arrhythmogenic substrate. For example, a study by Lu et  
404 al (2011)(23) suggests collagen can directly modulate the  $\text{Ca}^{2+}$  dynamics and electrical activities of  
405 atrial cardiomyocytes. Electrical and/or mechanical coupling can be disrupted if the extracellular  
406 matrix and cytoskeletal links are altered by increased integrin signalling (52) and this may also  
407 contribute to the HCM phenotype.

408  
409  *$\text{Ca}^{2+}$  transients*

410 When the young ACTC E99K mice were compared with NTG mice the most striking observation  
411 was that the hypercontractility due to the intrinsically higher  $\text{Ca}^{2+}$  sensitivity in mutant mice was  
412 accompanied by an *increased*  $\text{Ca}^{2+}$ -transient which would magnify the hypercontractile state of the  
413 TG mice.

414 It is interesting to note that the values for the  $\text{Ca}^{2+}$ -transient magnitude were distributed over a wide  
415 range of values and appeared to consist of two populations, one with a range similar to the wild-  
416 type plus 20-30% with values considerably higher that may correspond to the mice destined for  
417 SCD.

418 The observations that SR load is no different and diastolic  $[\text{Ca}^{2+}]$  less in the TG hearts yet the  $\text{Ca}^{2+}$   
419 transient amplitude is greater, implies there is an increase in trigger  $\text{Ca}^{2+}$ , or that excitation-  
420 contraction coupling is more sensitive due to a lowering of the threshold for  $\text{Ca}^{2+}$  activation either  
421 on the cytoplasmic(33) or luminal(13) sides of the ryanodine receptor (RyR). In hypertrophic  
422 cardiomyopathies it is not known if RyR  $\text{Ca}^{2+}$  activation thresholds change but such alterations in  
423 RyR properties may arise from abnormal expression of associated proteins e.g. calsequestrin,  
424 junctin and triadin(14) or changes in phosphorylation status(51). Increased RyR-mediated  $\text{Ca}^{2+}$   
425 leak from the SR is observed in HF in humans(58) and various animal models(22; 24; 44) though  
426 the underlying pathogenesis remains highly controversial(17).

427 In contrast, cardiac myocytes from the older 8-12 week TG animals showed no differences in  
428 maximum sarcomere shortening compared with their NTG counterparts but the  $\text{Ca}^{2+}$  transients  
429 were smaller. The attainment of similar shortening amplitude with less  $\text{Ca}^{2+}$  delivery derives from  
430 the hypercontractile nature of the ACTC E99K myocytes. This is a similar finding to most studies  
431 using TG mice with HCM mutations reporting results from adult mice (e.g. 4-6 months old(15; 19)  
432 or more elderly(48)). The evidence for abnormal  $\text{Ca}^{2+}$  transients associated with HCM mutations  
433 is equivocal and appears to be mutation-specific. Cardiac myocytes isolated from TG mice with a  
434 troponin T (TnT) mutation that is associated with a high risk of SCD in patients ( $\Delta\text{E160}$ ) had a  
435 decreased resting  $[\text{Ca}^{2+}]$  and larger and faster  $\text{Ca}^{2+}$  transients(19), but other TnT mutations (TnT  
436 R92L which is not linked with SCD, and TnT I79N which is associated with a high incidence of  
437 SCD) did not show these changes. The decreased  $\text{Ca}^{2+}$  transients in our older ACTC E99K TG

438 mouse hearts appear to provide compensation to normalise contraction hence preserve energy  
439 reserves in the face of the hypercontractile myofilaments and compromised ATP supply present at  
440 all ages(15; 19).

441 In previous work we reported that SCD in young ACTC E99K mice is more frequent in females  
442 than males(46). Many studies have recognized that there can be sex differences both in the onset  
443 and progression of cardiovascular diseases(31; 37; 39) and in cardiomyocyte intracellular  $\text{Ca}^{2+}$   
444 regulation (11; 54). Although we found very few sex differences in  $\text{Ca}^{2+}$  regulation we did find that  
445 the decay of the electrically-stimulated  $\text{Ca}^{2+}$  transient in female TG myocytes was slower than the  
446 transient decay in the male TG myocytes whereas there were no differences in decay time in the  
447 NTG cells. Differences in decay between males and females have also been noted in the rat by  
448 Leblanc et al (1998)(20) and Curl et al (2001)(6). We could not determine any sex differences in  
449 the TG mice in spark frequency or mass yet others have suggested possible sex-dependent  
450 alterations in RyR regulation(11). Therefore we can only state at this stage that sex differences in  
451 the TG mice are not large but they may contribute to the complex interactions occurring to produce  
452 the final phenotype.

#### 453 454 *$\text{Ca}^{2+}$ waves and arrhythmia provocation*

455 The consequence of the sensitised release process found in young TG mice is an alteration to the  
456 normal gating behaviour of the RYRs which cause aberrant activation of the channels as  
457 evidenced by the increased frequency and larger amplitudes and masses of  $\text{Ca}^{2+}$  sparks recorded  
458 in the myocytes isolated from young TG hearts. As with the  $\text{Ca}^{2+}$  transient amplitude there is a  
459 wide dispersal of values and evidence of two populations, whilst  $\text{Ca}^{2+}$  sparks recorded in the  
460 myocytes isolated from NTG and adult TG hearts do not appear to have different characteristics.  
461 With maintained SR  $\text{Ca}^{2+}$  content(53) the larger spontaneous  $\text{Ca}^{2+}$  release events in the young TG  
462 hearts translate into the increased appearance of  $\text{Ca}^{2+}$  waves(5; 9; 55).

463 It is well-described that the appearance of waves will activate the electrogenic  $\text{Na}^+/\text{Ca}^{2+}$   
464 exchange(12; 32) producing an inward current which can depolarise the cell. If a large fraction of  
465 the total SR  $\text{Ca}^{2+}$  content is released in producing the wave, the resultant delayed  
466 afterdepolarisation can be large enough to initiate an ectopic triggered action potential(32) that  
467 could generate arrhythmias and provoke spatially discordant alternans(56). The factors affecting  
468 source-sink mismatches that tend to cause after-depolarizations to be suppressed are unknown  
469 but such mismatches may be overcome by microfibrosis and structural remodelling(57), so  
470 allowing conduction spread. We hypothesise that while the disturbed single myocyte  $\text{Ca}^{2+}$  handling  
471 may initiate potentially arrhythmic depolarisations, changes in the passive properties of the heart  
472 tissue could allow such triggering events to develop and propagate(7), slow conduction and  
473 promote re-entry(36).

474

475 *Age and mouse strain determine sudden cardiac death.*

476 The occurrence of SCD in a time window centred on 36-40 days in the *ACTC* E99K and the *TNNI3*  
477 R193H TG mouse studied by Li et al.(21) indicates that important changes occur at this stage in  
478 development. This age corresponds to the end of a growth spurt whereby the heart and body  
479 weight increase 3.8-fold and 3.5-fold respectively between P10 and P35, reaching 80% of final  
480 body weight but only 70% of final heart weight and is immediately followed by puberty(35).

481 Although evidence suggests that transverse tubules systems and EC coupling mechanisms are  
482 fully developed by P20 in mice(41), there may not yet be appropriate adaptation to the intrinsically  
483 high myofibrillar  $\text{Ca}^{2+}$ -sensitivity leaving the TG mouse heart particularly vulnerable at this age.  
484 Studies grouped around this time should be more informative than those involving older animals in  
485 which complex secondary changes may have occurred that could mask initial triggers for HCM.

486 It is evident that some of the young mice have a hypercontractile phenotype associated with the  
487 increased  $\text{Ca}^{2+}$  transients and spark volumes whilst the TG survivors are not very different from  
488 their NTG littermates. Does this indicate that compensatory changes develop in adult mice or are  
489 there two populations of mice in our studies? The following observations would suggest that the  
490 latter possibility seems likely. The Kaplan-Meier plots of TG mouse survival show that not all  
491 animals die suddenly and, moreover, there is a striking dependence on the genetic background of  
492 the mice studied. There is very little SCD on a pure C57Bl6 background and more SCD on a  
493 CBA/Ca-enriched background compared with the hybrid C56Bl6xCBA/Ca. In every generation of  
494 hybrid mice two populations of mice are consistently observed – those that die suddenly and those  
495 that do not – despite the same level of expression of the mutant actin protein in both populations  
496 (see Figure 1 and ref (46)). The survivors have a similar lifespan to the NTG animals. The SCD  
497 phenotype correlates with an obvious fraction of cells isolated from the hearts of young TG animals  
498 that have larger  $\text{Ca}^{2+}$  transients, larger spark masses and more  $\text{Ca}^{2+}$  waves suggesting  
499 segregation of phenotypes when the TG mice are bred on a hybrid C57Bl6 x CBA/Ca genetic  
500 background. These are properties not shared by the survivors or the NTG animals, suggesting  
501 that the animals with high spark mass are destined for SCD.

502 This is supported by results with the *ACTC* E99K transgene bred onto a pure C57Bl6 background,  
503 where both young and old TG mice showed the same spark mass as NTG littermates,  
504 corresponding to the absence of SCD; thus it is the genetically-determined secondary response to  
505 the initial mutation-induced abnormality that is crucial for provoking SCD. The C57Bl6 haplotype is  
506 known to be resistant to arrhythmia provocation and angiotensin-induced myopathy whilst the  
507 CBA/Ca is genetically closer to mouse strains that show much more susceptibility to arrhythmias  
508 e.g BalbC(26; 38).

509 The underlying mechanism is not known. This may take place because of subtleties in dyad  
510 architecture, energy or phosphorylation status. Alternatively, the primed pro-arrhythmic substrate  
511 orchestrated by  $\text{Ca}^{2+}$  dysregulation in the TG mice may be activated by structural changes, such as

512 fibrosis, that could occur in parallel and be genetically determined, for example the T-helper cell  
513 genotypes 1 and 2 and their role in cardiac remodelling(38).

514 It is particularly interesting that the influence of genetic background on the manifestation of the  
515 SCD trait due to the *ACTC* E99K mutation parallels the well known variability of penetrance in  
516 families with the same HCM-linked mutation. Indeed a study of 76 individuals from 11 families with  
517 the *ACTC* E99K mutation revealed SCD in 8 cases but 5 of these were in the same family(34; 46).  
518 The ability to reproduce variable penetrance of SCD in a mouse model could enable us to  
519 determine the background factors that determine pathogenicity.

520

521 **Grants**

522 This work was supported by British Heart Foundation Programme Grant [grant number  
523 PG11/020/29266] and a BHF PhD studentship [grant number FS10/021/20244].

524

525 **Disclosures**

526 None

527

528 **Acknowledgements**

529 We acknowledge the technical assistance of O'Neal Copeland for producing the Western blot data  
530 summarised in Figure 1.

531

532

533

534

535

536

537

538

539

540

541

542

543

544

545

546

547

548

549



550 **Reference List**

- 551
- 552 1. **Alfares AA, Kelly MA, McDermott G, Funke BH, Lebo MS, Baxter SB, Shen J,**
- 553 **McLaughlin HM, Clark EH, Babb LJ, Cox SW, DePalma SR, Ho CY, Seidman JG,**
- 554 **Seidman CE and Rehm HL.** Results of clinical genetic testing of 2,912 probands with
- 555 hypertrophic cardiomyopathy: expanded panels offer limited additional sensitivity. *Genetics in*
- 556 *Medicine* 17: 880-888, 2015.
- 557 2. **Bassani JWM, Bassani RA and Bers DM.** Relaxation in rabbit and rat cardiac cells:
- 558 species-dependent differences in cellular mechanisms. *J Physiol* 476: 279-293, 1994.
- 559 3. **Baudenbacher F, Schober T, Pinto JR, Sidorov VY, Hilliard F, Solaro RJ, Potter JD and**
- 560 **Knollmann B.** Myofilament  $\text{Ca}^{2+}$  sensitization causes susceptibility to cardiac arrhythmia in
- 561 mice. *J Clin Invest* 118: 3893-3903, 2008.
- 562 4. **Bers DM.** *Excitation-contraction coupling and cardiac contractile force.* Dordrecht: Kluwer
- 563 Academic, 2001.
- 564 5. **Cheng H, Lederer MR, Lederer WJ and Cannell MB.** Calcium sparks and  $[\text{Ca}^{2+}]_i$  waves in
- 565 cardiac myocytes. *Am J Physiol* 270: C148-C159, 1996.
- 566 6. **Curl CL, Wendt IR and Kotsanas G.** Effects of gender on intracellular  $[\text{Ca}^{2+}]$  in rat cardiac
- 567 myocytes. *Pflügers Arch* 441: 709-716, 2001.
- 568 7. **de Jong S, van Veen TAB, van Rijen HVM and de Bakker JMT.** Fibrosis and cardiac
- 569 arrhythmias. *J Cardiovasc Pharmacol* 57: 630-638, 2011.
- 570 8. **Diaz ME, Trafford AW, O'Neill SC and Eisner DA.** Measurement of sarcoplasmic reticulum
- 571  $\text{Ca}^{2+}$  content and sarcolemma  $\text{Ca}^{2+}$  fluxes in isolated rat ventricular myocytes during
- 572 spontaneous  $\text{Ca}^{2+}$  release. *J Physiol* 501: 3-16, 1997.

- 573 9. **Eisner DA and Valdeolmillos M.** A study of intracellular calcium oscillations in sheep  
574 cardiac Purkinje fibres measured at the single cell level. *J Physiol* 372: 539-556, 1986.
- 575 10. **Escobar AL, Ribeiro-Costa R, Villalba-Galea C, Zoghbi ME, Pérez CG and Mejía-Alvarez**  
576 **R.** Developmental changes of intracellular  $\text{Ca}^{2+}$  transients in beating rat hearts. *Am J Physiol*  
577 286: H971, 2004.
- 578 11. **Farrell SR, Ross JL and Howlett SE.** Sex differences in mechanisms of cardiac excitation-  
579 contraction coupling in rat ventricular myocytes. *Am J Physiol* 299: H36-H45, 2010.
- 580 12. **Fedida D, Noble D, Rankin AC and Spindler AJ.** The arrhythmogenic transient inward  
581 current  $i_{\text{Ti}}$  and related contraction in isolated guinea-pig ventricular myocytes. *J Physiol*  
582 392: 523-542, 1987.
- 583 13. **Gyorke I and Györke S.** Regulation of the cardiac ryanodine receptor channel by luminal  
584  $\text{Ca}^{2+}$  involves luminal  $\text{Ca}^{2+}$  sensing sites. *Biophys J* 75: 2801-2810, 1998.
- 585 14. **Gyorke S and Terentyev D.** Modulation of ryanodine receptor by luminal calcium and  
586 accessory proteins in health and cardiac disease. *Cardiovasc Res* 77: 245-255, 2008.
- 587 15. **Haim TE, Dowell C, Diamanti T, Scheuer J and Tardiff JC.** Independent FHC-related  
588 cardiac troponin T mutations exhibit specific alterations in myocellular contractility and  
589 calcium kinetics. *J Mol Cell Cardiol* 42: 1098-1110, 2007.
- 590 16. **Hollingworth S, Peet J, Chandler WK and Baylor SM.** Calcium sparks in intact skeletal  
591 muscle fibers of the frog. *J Gen Physiol* 118: 653-678, 2001.

- 592 17. **Houser SR.** Controversies in Cardiovascular Research: Role of protein kinase A mediated  
593 hyperphosphorylation of the ryanodine receptor at serine 2808 in heart failure and  
594 arrhythmias. *Circ Res* 114: 1320-1327, 2014.
- 595 18. **Huke S and Knollmann BC.** Increased myofilament  $\text{Ca}^{2+}$ -sensitivity and arrhythmia  
596 susceptibility. *J Mol Cell Cardiol* 48: 824-833, 2010.
- 597 19. **Knollmann BC, Kirchhof P, Sirenko SG, Degen H, Greene AE, Schober T, Mackow JC,**  
598 **Fabritz L, Potter JD and Morad M.** Familial hypertrophic cardiomyopathy-linked mutant  
599 troponin T causes stress-induced ventricular tachycardia and  $\text{Ca}^{2+}$ -dependent action potential  
600 remodeling. *Circ Res* 92: 428-436, 2003.
- 601 20. **Leblanc N, Chartier D, Gosselin H and Rouleau JL.** Age and gender differences in  
602 excitation-contraction coupling of the rat ventricle. *J Physiol* 511: 533-548, 1998.
- 603 21. **Li Y, Zhang L, Jean-Charles PY, Nan C, Chen G, Tian J, Jin JP, Gelb IJ and Huang X.**  
604 Dose-dependent diastolic dysfunction and early death in a mouse model with cardiac  
605 troponin mutations. *J Mol Cell Cardiol* 62: 227-236, 2013.
- 606 22. **Louch W, Hake J, Mørk H, Hougen K, Skrbic B, Ursu D, Tønnessen T, Sjaastad I and**  
607 **Sejersted O.** Slow  $\text{Ca}^{2+}$  sparks de-synchronize  $\text{Ca}^{2+}$  release in failing cardiomyocytes:  
608 evidence for altered configuration of  $\text{Ca}^{2+}$  release units? *J Mol Cell Cardiol* 58: 41-52, 2013.
- 609 23. **Lu YY, Chen YC, Kao YH, Wu TJ, Chen SA and Chen YJ.** Extracellular matrix of collagen  
610 modulates intracellular calcium handling and electrophysiological characteristics of HL-1  
611 cardiomyocytes with activation of angiotensin II type 1 receptor. *J Cardiac Fail* 17: 82-90,  
612 2011.

- 613 24. **Lyon A, MacLeod K, Zhang Y, Hayward C, Kanda G, Lab M, Korchev Y, Harding S and**  
614 **Gorelik J.** Loss of T-tubules and other changes to surface topography in ventricular  
615 myocytes from failing human and rat heart. *Proc Natl Acad Sci USA* 106: 6854-6859, 2009.
- 616 25. **MacLeod KT and Harding SE.** Effects of phorbol ester on contraction, intracellular pH and  
617 intracellular  $\text{Ca}^{++}$  in isolated mammalian ventricular myocytes. *J Physiol* 444: 481-498, 1991.
- 618 26. **Maguire CT, Wakimoto H, Patel VV, Hammer PE, Gauvreau K and Berul CI.** Implications  
619 of ventricular arrhythmia vulnerability during murine electrophysiology studies. *Physiol*  
620 *Genomics* 15: 84-91, 2003.
- 621 27. **Maron BJ.** Hypertrophic cardiomyopathy: a systematic review. *J Am Med Assoc* 287: 1308-  
622 1320, 2002.
- 623 28. **Maron BJ, McKenna WJ, Danielson GK, Kappenberger LJ, Kuhn HJ, Seidman CE, Shah**  
624 **PM, Spencer WH, Spirito P, ten Cate FJ, Wigle ED, Vogel RA, Abrams J, Bates ER,**  
625 **Brodie BR, Danias PG, Gregoratos G, Hlatky MA, Hochman JS, Kaul S, Lichtenberg**  
626 **RC, Lindner JR, O'Rourke RA, Pohost GM, Schofield RS, Tracy CM, Winters WL, Klein**  
627 **WW, Priori SG, Alonso-Garcia A, Blomström-Lundqvist C, De Backer G, Deckers J,**  
628 **Flather M, Hradec J, Oto A, Parkhomenko A, Silber S and Torbicki A.** American College  
629 of Cardiology/European Society of Cardiology Clinical Expert Consensus Document on  
630 Hypertrophic Cardiomyopathy. *Eur Heart J* 24: 1965-1991, 2003.
- 631 29. **Marston S.** Why is there a limit to the changes in myofilament  $\text{Ca}^{2+}$ -sensitivity associated  
632 with myopathy causing mutations? *Frontiers in Physiology* 7: 415, 2016.
- 633 30. **Marston S.** How do mutations in contractile proteins cause the primary familial  
634 cardiomyopathies? *J Cardiovasc Trans Res* 4: 245-255, 2011.

- 635 31. **Martínez-Sellés M, Doughty RN, Poppe K, Whalley GA, Earle N, Tribouilloy C,**  
636 **McMurray JJV, Swedberg K, Køber L, Berry C, Squire I and on behalf of the Meta-**  
637 **Analysis Global Group In Chronic Heart Failure (MAGGIC).** Gender and survival in  
638 patients with heart failure: interactions with diabetes and aetiology. Results from the MAGGIC  
639 individual patient meta-analysis. *Eur J Heart Fail* 14: 473-479, 2012.
- 640 32. **Mechmann S and Pott L.** Identification of Na-Ca exchange current in single cardiac  
641 myocytes. *Nature* 319: 597-599, 1986.
- 642 33. **Meissner G and Henderson JS.** Rapid Ca release from cardiac sarcoplasmic reticulum  
643 vesicles is dependent on  $\text{Ca}^{2+}$  and is modulated by  $\text{Mg}^{2+}$ , adenine nucleotide and calmodulin.  
644 *J Biol Chem* 262: 3065-3073, 1987.
- 645 34. **Monserat L, Hermida-Prieto M, Fernandez X, Rodríguez I, Dumont C, Cazón L, Cuesta**  
646 **MG, Gonzalez-Juanatey C, Peteiro J, Álvarez N, Penas-Lado M and Castro-Beiras A.**  
647 Mutation in the alpha-cardiac actin gene associated with apical hypertrophic cardiomyopathy,  
648 left ventricular non-compaction, and septal defects. *Eur Heart J* 28: 1953-1961, 2007.
- 649 35. **Naqvi N, Li M, Calvert JW, Tejada T, Lambert JP, Wu J, Kesteven SH, Holman SR,**  
650 **Matsuda T, Lovelock JD, Howard WW, Iismaa SE, Chan AY, Crawford BH, Wagner MB,**  
651 **Martin DI, Lefer DJ, Graham RM and Husain A.** A proliferative burst during preadolescence  
652 establishes the final cardiomyocyte number. *Cell* 157: 795-807, 2014.
- 653 36. **Nguyen TP, Qu Z and Weiss JN.** Cardiac fibrosis and arrhythmogenesis: The road to repair  
654 is paved with perils. *J Mol Cell Cardiol* 70: 83-91, 2014.
- 655 37. **Nieminen MS, Harjola VP, Hochadel M, Drexler H, Komajda M, Brutsaert D, Dickstein K,**  
656 **Ponikowski P, Tavazzi L, Follath F and Lopez-Sendon JL.** Gender related differences in

- 657 patients presenting with acute heart failure. Results from EuroHeart Failure Survey II. *Eur J*  
 658 *Heart Fail* 10: 140-148, 2008.
- 659 38. **Peng H, Yang XP, Carretero OA, Nakagawa P, D'Ambrosio M, Leung P, Xu J, Peterson**  
 660 **EL, González GE, Harding P and Rhaleb NE.** Angiotensin II-induced dilated  
 661 cardiomyopathy in Balb/c but not C57BL/6J mice. *Exp Physiol* 96: 756-764, 2011.
- 662 39. **Petrie MC, Dawson NF, Murdoch DR, Davie AP and McMurray JJV.** Failure of women's  
 663 hearts. *Circ* 99: 2334-2341, 1999.
- 664 40. **Picht E, Zima AV, Blatter LA and Bers DM.** SparkMaster: automated calcium spark  
 665 analysis with ImageJ. *Am J Physiol* 293: C1073-C1081, 2007.
- 666 41. **Reynolds JO, Chiang DY, Wang W, Beavers DL, Dixit SS, Skapura DG, Landstrom AP,**  
 667 **Song LS, Ackerman MJ and Wehrens XH.** Junctophilin-2 is necessary for T-tubule  
 668 maturation during mouse heart development. *Cardiovasc Res* 100: 44-53, 2013.
- 669 42. **Satoh H, Blatter LA and Bers DM.** Effects of  $[Ca^{2+}]_i$ , SR  $Ca^{2+}$  load, and rest on  $Ca^{2+}$  spark  
 670 frequency in ventricular myocytes. *Am J Physiol* 272: H657-H668, 1997.
- 671 43. **Seki S, Nagashima M, Yamada Y, Tsutsuura M, Kobayashi T, Namiki A and Tohse N.**  
 672 Fetal and postnatal development of  $Ca^{2+}$  transients and  $Ca^{2+}$  sparks in rat cardiomyocytes.  
 673 *Cardiovasc Res* 58: 535-548, 2003.
- 674 44. **Shannon TR, Pogwizd SM and Bers DM.** Elevated sarcoplasmic reticulum  $Ca^{2+}$  leak in  
 675 intact ventricular myocytes from rabbits in heart failure. *Circ Res* 93: 592-594, 2003.

- 676 45. **Sikkel MB, Collins TP, Rowlands C, Shah M, O'Gara P, Williams AJ, Harding SE, Lyon**  
677 **AR and MacLeod KT.** Flecainide reduces Ca(2+) spark and wave frequency via inhibition of  
678 the sarcolemmal sodium current. *Cardiovasc Res* 98: 286-296, 2013.
- 679 46. **Song W, Dyer E, Stuckey DJ, Copeland O'N, Leung MC, Bayliss C, Messer A, Wilkinson**  
680 **R, Tremoleda JL, Schneider MD, Harding SE, Redwood CS, Clarke K, Nowak K,**  
681 **Montserrat L, Wells D and Marston SB.** Molecular mechanism of the E99K mutation in  
682 cardiac actin (ACTC gene) that causes apical hypertrophy in man and mouse. *J Biol Chem*  
683 286: 27582-27593, 2011.
- 684 47. **Song W, Vikhorev PG, Kashyap MN, Rowlands C, Ferenczi MA, Woledge RC, Macleod**  
685 **K, Marston S and Curtin NA.** Mechanical and energetic properties of papillary muscle from  
686 ACTC E99K transgenic mouse models of hypertrophic cardiomyopathy. *Am J Physiol* 304:  
687 H1513-H1524, 2013.
- 688 48. **Spindler M, Saupe KW, Christe ME, Sweeney HL, Seidman CE, Seidman JG and Ingwall**  
689 **JS.** Diastolic dysfunction and altered energetics in the alphaMHC403/+ mouse model of  
690 familial hypertrophic cardiomyopathy. *J Clin Invest* 101: 1775-1783, 1998.
- 691 49. **Tanaka H and Shigenoby K.** Effect of ryanodine on neonatal and adult rat heart:  
692 developmental increase in sarcoplasmic reticulum function. *J Mol Cell Cardiol* 21: 1305-1313,  
693 1989.
- 694 50. **Terracciano CMN, De Souza AI, Philipson KD and MacLeod KT.** Na/Ca exchange and  
695 sarcoplasmic reticular Ca regulation in ventricular myocytes from transgenic mice  
696 overexpressing the Na/Ca exchange. *J Physiol* 512: 615-676, 1998.
- 697 51. **Ullrich ND, Valdivia HH and Niggli E.** PKA phosphorylation of cardiac ryanodine receptor  
698 modulates SR luminal Ca<sup>2+</sup> sensitivity. *J Mol Cell Cardiol* 53: 33-42, 2012.

- 699 52. **Valencik ML, Zhang D, Punske B, Hu P, McDonald JA and Litwin SE.** Integrin activation  
700 in the heart. *Circ Res* 99: 1403, 2006.
- 701 53. **Venetucci LA, Trafford AW and Eisner DA.** Increasing ryanodine receptor open probability  
702 alone does not produce arrhythmogenic calcium waves: threshold sarcoplasmic reticulum  
703 calcium content is required. *Circ Res* 100: 105-111, 2007.
- 704 54. **Wasserstrom JA, Kapur S, Jones S, Faruque T, Sharma R, Kelly JE, Pappas A, Ho W,**  
705 **Kadish AH and Aistrup GL.** Characteristics of intracellular  $\text{Ca}^{2+}$  cycling in intact rat heart: a  
706 comparison of sex differences. *Am J Physiol* 295: H1895-H1904, 2008.
- 707 55. **Wier WG, Cannell MB, Berlin JR, Marban E and Lederer WJ.** Cellular and subcellular  
708 heterogeneity of  $[\text{Ca}^{2+}]_i$  in single heart cells revealed by fura-2. *Science* 235: 325-328, 1987.
- 709 56. **Xie LH and Weiss JN.** Arrhythmogenic consequences of intracellular calcium waves. *Am J*  
710 *Physiol* 297: H997-H1002, 2009.
- 711 57. **Xie Y, Sato D, Garfinkel A, Qu Z and Weiss JN.** So little source, so much sink:  
712 requirements for afterdepolarizations to propagate in tissue. *Biophys J* 99: 1408-1415, 2010.
- 713 58. **Zhang C, Chen B, Guo A, Zhu Y, Miller JD, Gao S, Yuan C, Kutschke W, Zimmerman K,**  
714 **Weiss RM, Wehrens XH, Hong J, Johnson FL, Santana LF, Anderson ME and Song LS.**  
715 Microtubule-mediated defects in junctophilin-2 trafficking contribute to myocyte T-tubule  
716 remodeling and  $\text{Ca}^{2+}$  handling dysfunction in heart failure. *Circ* 129: 1742-1750, 2014.  
717  
718  
719



## 720 **Figure legends**

721

722 *Figure 1* – Quantification of transgene expression by Western blots with antibody specific to the  
723 E99K mutation. Upper panel: Western blot and corresponding whole protein stained membrane.  
724 Lower panel: time dependence of level of E99K expressed relative to adult.

725

726 *Figure 2* – Panels A - C show representative histological sections of hearts from (A) NTG, (B)  
727 *ACTC* E99K TG mice and (C) *ACTC* E99K TG mice that suffered sudden cardiac death. Picrosirius  
728 stained heart sections (for collagen determination) are shown in the left panels and wheatgerm  
729 agglutinin sections (for cell cross-sectional area measurements) are shown in the right panels.  
730 Panel D shows the mean ( $\pm$  SEM) cross-sectional area of myocytes from sections similar to those  
731 shown in Panels A, B and C. More than 690 myocytes were analysed from each group. Panel E  
732 shows the mean ( $\pm$  SEM) percentage of the field of view that stains positively for collagen with  
733 picrosirius red. These data were acquired from 3 NTG hearts, 4 TG hearts, 2 hearts from TG mice  
734 that suffered sudden cardiac death and 3 NTG and 3 TG hearts from mice on a pure C57Bl6  
735 background. Panels F and G show the differences in *COL1A1* and *COL3A1* mRNA levels  
736 respectively in NTG, TG and SCD hearts. *COL1A1* encodes the pro- $\alpha$ 1 chains of type I  
737 collagen and *COL3A1* encodes the pro- $\alpha$ 1 chains of type III collagen. Panel F shows the  
738 means  $\pm$  SEM ( $n > 6$ ); ANOVA with Tukey's multiple comparison test; \* =  $P < 0.05$ , \*\* =  $P < 0.01$ .  
739 Panel G shows the means  $\pm$  SEM ( $n = 3$ ).

740

741 *Figure 3* – Contraction and  $\text{Ca}^{2+}$  transients in young (25-45 days) (left panels) and adult (8-12  
742 weeks) (right panels) mice. The top panels (A and B) show typical traces of contraction profiles  
743 (expressed in terms of sarcomere length changes) of NTG (dotted line) and TG (solid line) cells.  
744 Corresponding pooled sarcomere shortening data (means  $\pm$  SEM) is shown in the right hand  
745 graphs. Panels C and D show typical traces of  $\text{Ca}^{2+}$  transients of NTG (dotted line) and TG (solid  
746 line) cells and the corresponding pooled data (means  $\pm$  SEM) on the right of the traces for the  
747 young and adult mice respectively. Mean data calculated from 92 cells isolated from 10 NTG  
748 young animals, 77 cells from 8 TG young animals, 64 cells isolated from 10 NTG adult animals and  
749 41 cells from 8 TG adult animals. \*\*\* =  $P < 0.001$ , \*\* =  $P < 0.01$ , T-test. Panels E and F show  
750 scatter graphs of  $\text{Ca}^{2+}$  transient amplitudes recorded from young (Panel E) TG (■) and NTG (□)  
751 and adult (Panel F) TG (■) and NTG (□) cardiac myocytes. The dashed lines indicate the  
752 greatest transient amplitude recorded from young NTG mice. Almost a quarter of the young TG  
753 cells had  $\text{Ca}^{2+}$  transient amplitudes greater than the largest transients observed in NTG cells.

754

755 *Figure 4* – Panel A shows typical traces of spontaneous contractile waves (denoted by arrows)  
756 occurring in NTG and TG cardiac myocytes isolated from young animals. These spontaneous  
757 contractions occurred during a quiescent 30 sec period following 1 Hz stimulation. Panel B shows

758 pooled data of wave frequency in the quiescent period in NTG and TG cells presented as mean  $\pm$   
759 SEM; n = 80 cells from 8 NTG animals, 80 cells from 9 TG animals. \*\*\* = P < 0.001. Panel C  
760 shows Ca<sup>2+</sup> waves in young cells recorded using Fura-2. Typical responses are shown for NTG  
761 (upper) and TG (lower) cells. Cells were paced at a particular frequency for 1 min then the  
762 stimulation train was stopped and spontaneous Ca<sup>2+</sup> waves recorded over the next 30 s. Panel D  
763 shows the effect of the stimulation train frequency on the occurrence of Ca<sup>2+</sup> waves in young  
764 NTG(□) and TG (■) cardiac myocytes. Data are presented as mean  $\pm$  SEM; n = 20 cells from 5  
765 NTG animals and 20 cells from 4 TG animals.

766

767 *Figure 5 – Wave-free survival of young TG and NTG myocytes following different pacing rates. The*  
768 *time to the first spontaneous contraction was measured as the time from the last electrically-*  
769 *stimulated contraction to the first spontaneous contraction. This was represented in a Kaplan-Meier*  
770 *survival curve. Upper panel shows survival following a 0.5 Hz train. Middle panel shows survival*  
771 *following a 2.0 Hz train and the lower panel shows survival following a 5.0 Hz train. Points are*  
772 *means calculated from 80 TG cells from 9 animals and 80 NTG cells from 8 animals.*

773

774 *Figure 6 – Determinations of SR Ca content in young and adult myocytes assessed using rapid*  
775 *application of 10 mM caffeine in a Na<sup>+</sup>-free / Ca<sup>2+</sup>-free solution (Panel A). Pooled data showing the*  
776 *differences in the SR Ca<sup>2+</sup> content of myocytes isolated from young (Panel B) and adult (Panel C)*  
777 *mice. Data are presented as mean  $\pm$  SEM; n = 56 cells from 10 young NTG animals, 25 cells from*  
778 *8 young TG animals. n = 34 cells from 10 adult NTG animals and 28 cells from 6 adult TG animals.*  
779 *\*\* = P < 0.01, T-test.*

780

781 *Figure 7 – Sex-based alterations in intracellular Ca<sup>2+</sup> regulation between cardiomyocytes isolated*  
782 *from surviving female and male ACTC E99K mice. The time to 50% decay of Ca<sup>2+</sup> transients*  
783 *evoked electrically (Panel A) and by rapid application of caffeine (Panel B). n = 46 cells from male*  
784 *NTG animals, 37 cells from male TG animals, 47 cells from female NTG animals and 42 cells from*  
785 *female TG animals \* = P < 0.05, \*\* = P < 0.01, ANOVA.*

786

787 *Figure 8 – Spark properties of cardiac myocytes isolated from young and adult TG and NTG*  
788 *hearts. Panel A shows typical line scan recordings of Ca<sup>2+</sup> sparks in young NTG and TG cells.*  
789 *Horizontal scale bar = 50  $\mu$ m, vertical scale bar = 500 ms. Scatter graphs of data for spark*  
790 *frequency and spark amplitude for young cells are shown in panels B and D with their*  
791 *corresponding log transforms in panels C and E. The bars on the scatter graphs indicate the*  
792 *means of these data. The log transforms are plotted with box (25<sup>th</sup> to 75<sup>th</sup> percentiles) and*  
793 *whiskers (entire range of data points). The line in the box signifies the median. Panels B, C, D and*  
794 *E show data from young hearts. NTG = 68 myocytes isolated from 5 hearts, TG = 60 myocytes*  
795 *isolated from 4 hearts. \*\*\* = P < 0.001, \*\* = P < 0.01. T-test. Panels F, G, H and I show data from*

adult hearts. The graphs are laid out in an identical way. Scatter graphs of data for spark frequency and spark amplitude for adult cells are shown in panels F and G with their corresponding log transforms in panels H and I. NTG = 70 myocytes isolated from 5 hearts, TG = 49 myocytes isolated from 3 hearts. \*\*\* =  $P < 0.001$ , T-test.

*Figure 9* – Spark masses measured in cardiac myocytes isolated from young (Panel A) and adult (Panel B) TG and NTG hearts with a mixed (hybrid) C57/Bl6 x CBA/Ca background. Panel C shows similar measurements on young NTG and E99K TG mice bred on a pure C57Bl6 background. The corresponding log transformations in box and whisker form are illustrated in panels B, D and F. The boxes represent the 25<sup>th</sup> to 75<sup>th</sup> percentiles and the whiskers the entire range of data points. The line in the box signifies the median. \*\*\* =  $P < 0.001$ , ANOVA with Bonferroni. For Panels A and B, NTG = 68 myocytes isolated from 5 hearts, TG = 60 myocytes isolated from 4 hearts. For Panels C and D, NTG = 70 myocytes isolated from 5 hearts, TG = 49 myocytes isolated from 3 hearts. For Panels E and F NTG = 75 myocytes isolated from 6 hearts, TG = 67 myocytes isolated from 8 hearts.

*Figure 10* – Left panel; Kaplan-Meier survival plots of each TG mouse line. The survival of the mixed hybrid TG mice (ie those with the C57/Bl6 x CBA/Ca background) is described by the solid line. The survival of mice bred on a pure C57Bl6 background is described by the dashed line and the survival of first generation TG mice bred on a pure CBA/Ca background showed the shortest survival duration indicated by the dotted line. Right panel; the distribution of age at death in the hybrid TG mice (n = 35).

**Table 1**  
Resting (diastolic) Fura-2 ratios

	Young (mean±SEM) (number of cells)		Adult (mean±SEM) (number of cells)	
Resting [Ca <sup>2+</sup> ] (Fura-2 ratio)	NTG 1.49±0.02 (109)	$P < 0.05$	NTG 1.41±0.01 (93)	$P < 0.01$
	TG 1.44±0.02 (69)		TG 1.29±0.01 (65)	

FIG 1

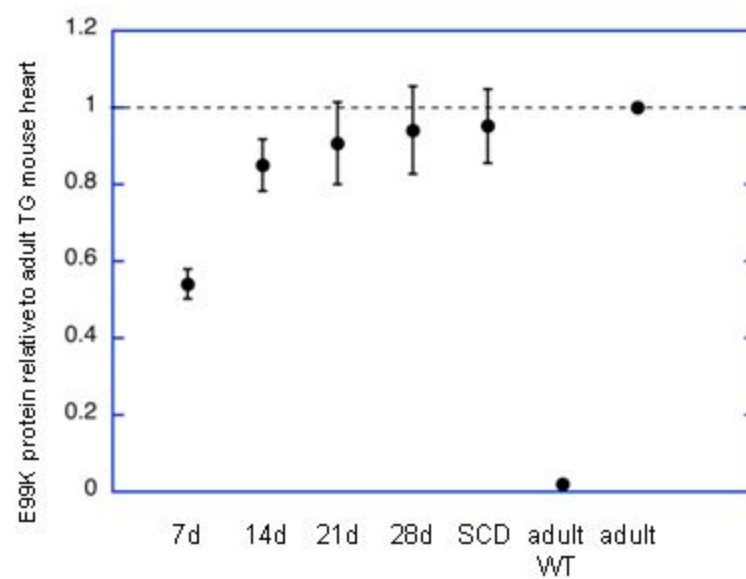
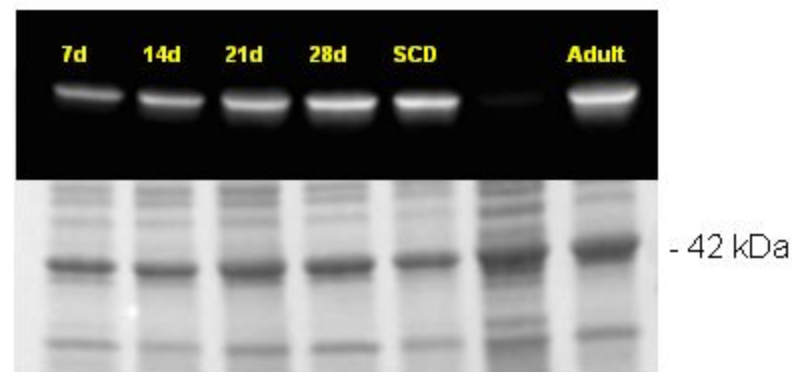
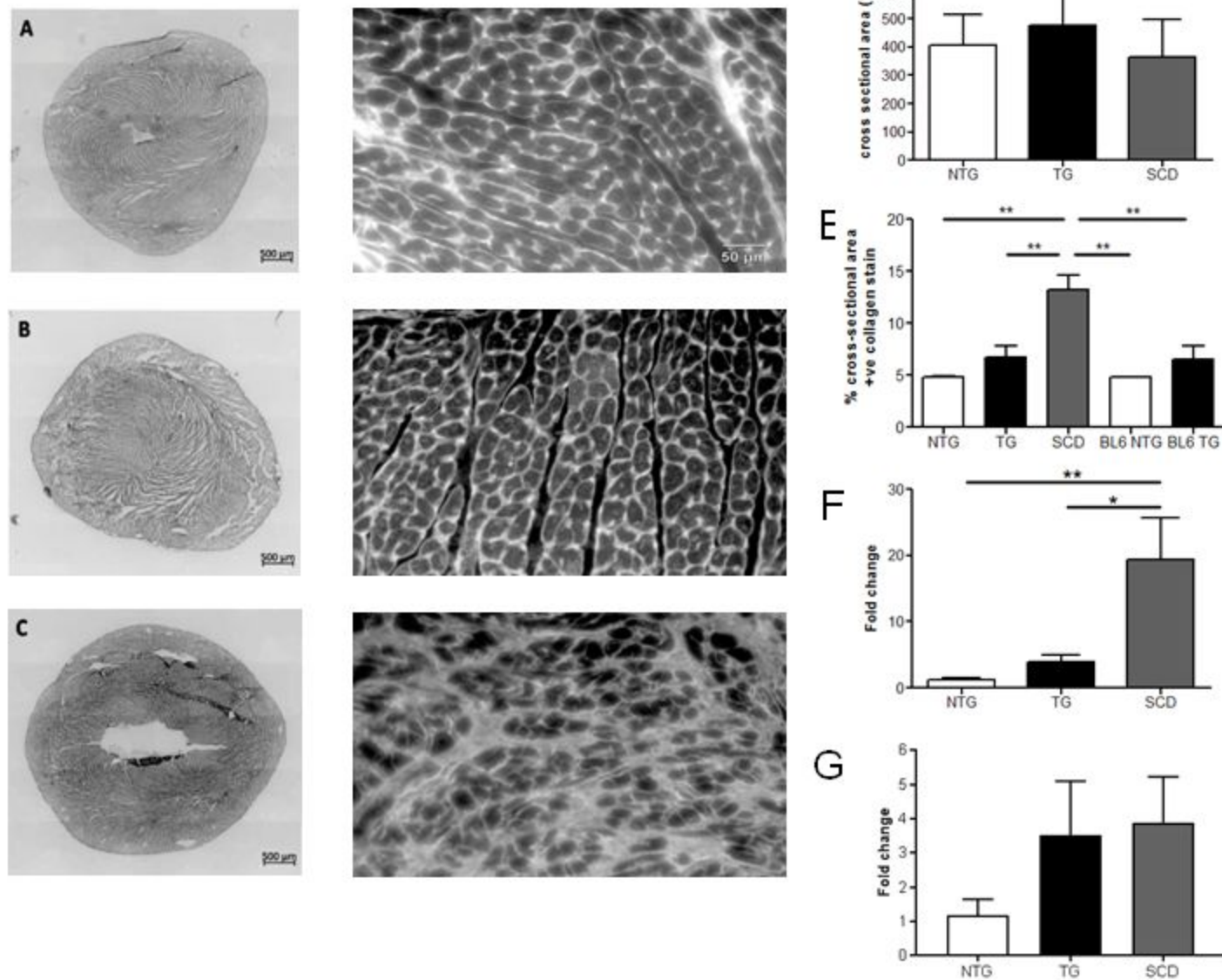


FIG 2

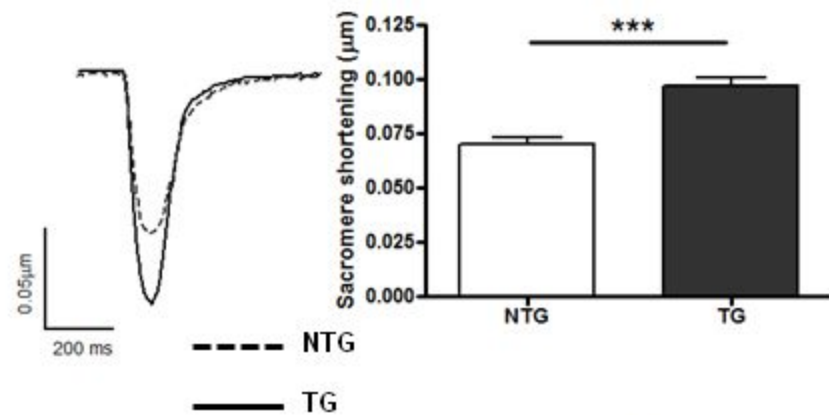


Young mice

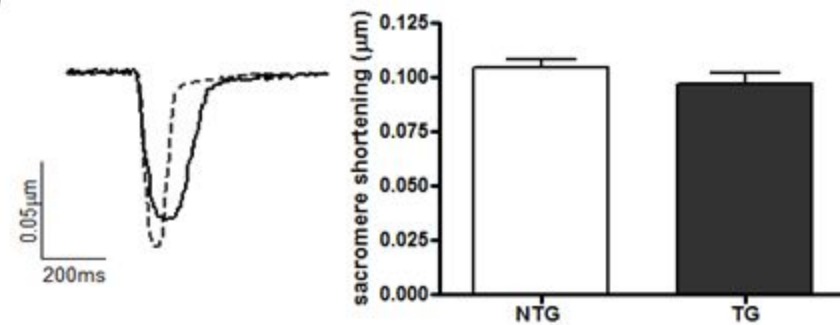
Adult mice

FIG 3

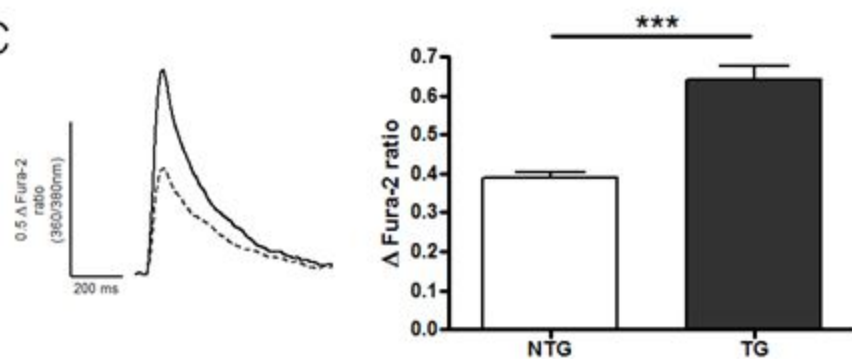
A



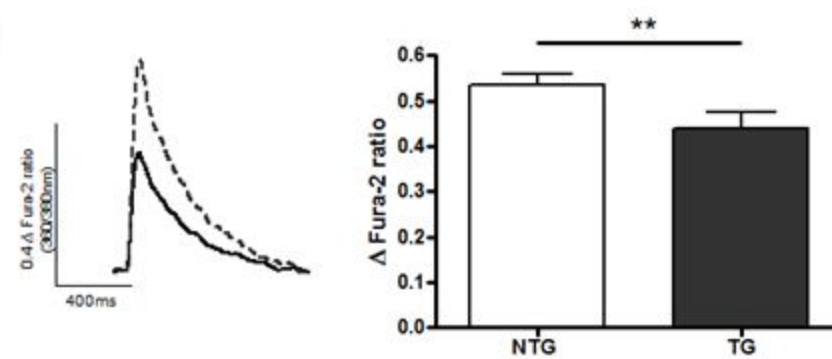
B



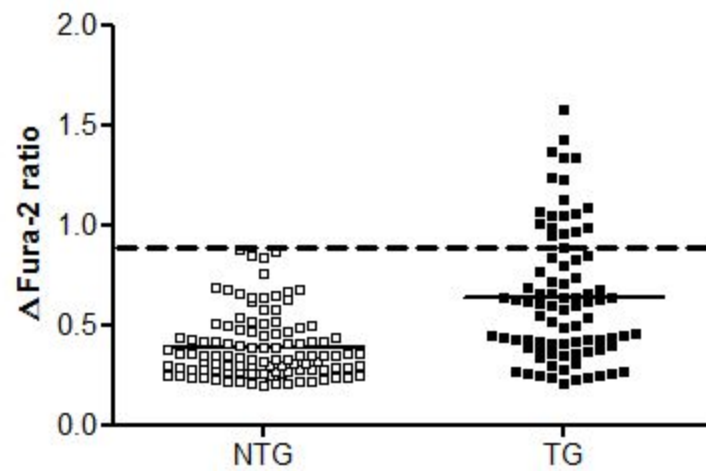
C



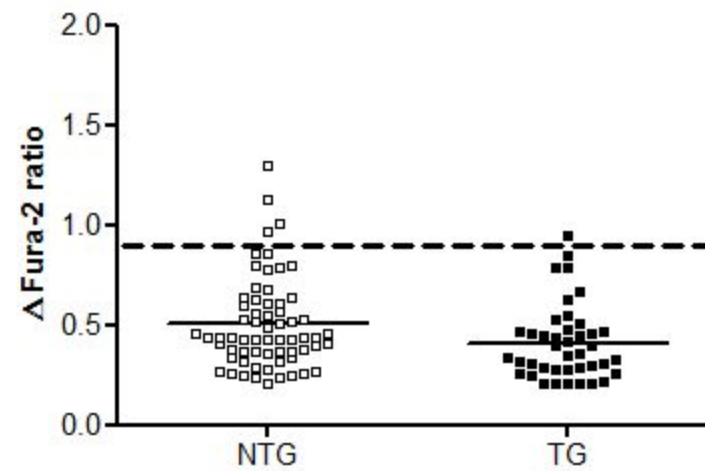
D



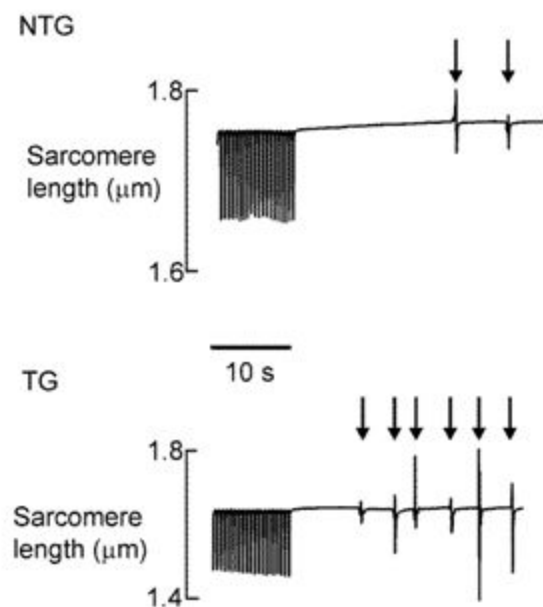
E



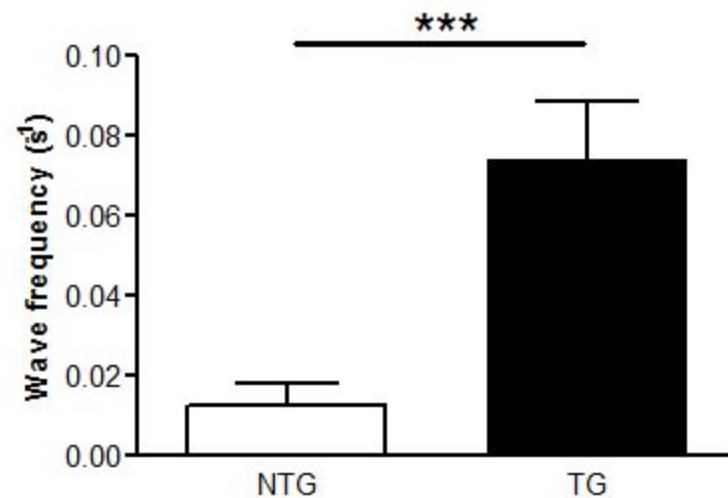
F



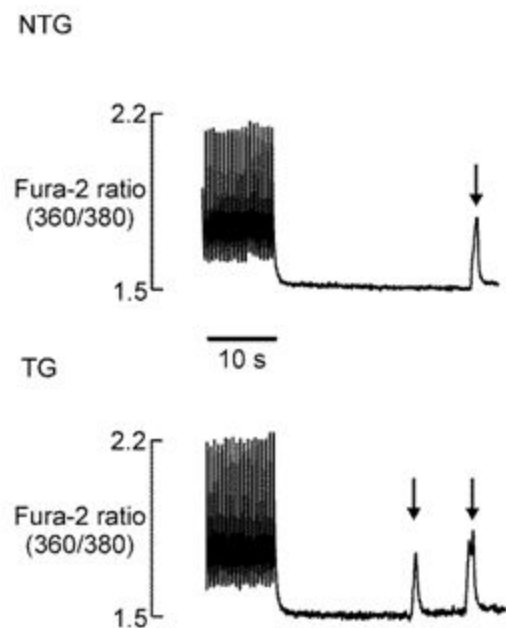
A



B



C



D

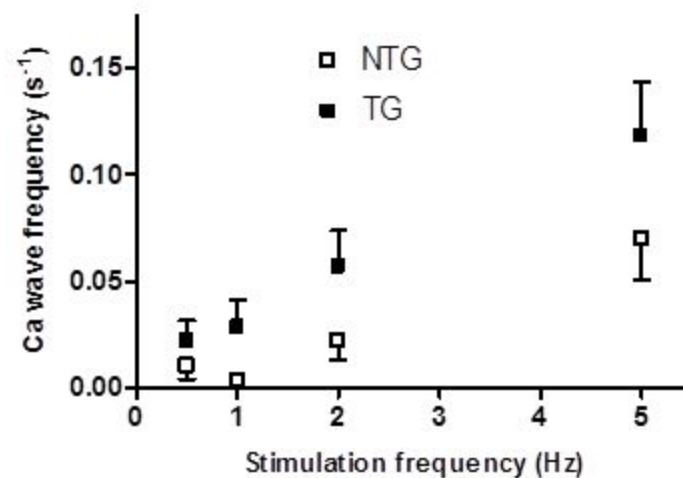
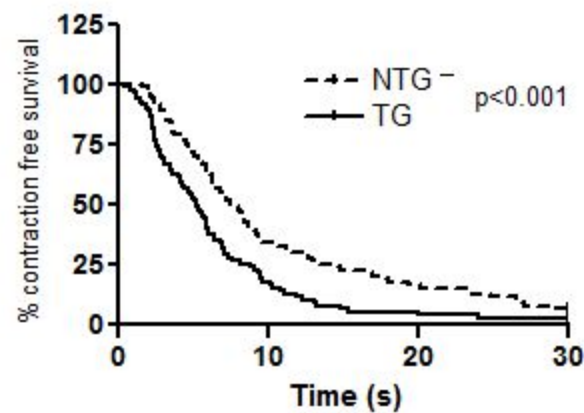
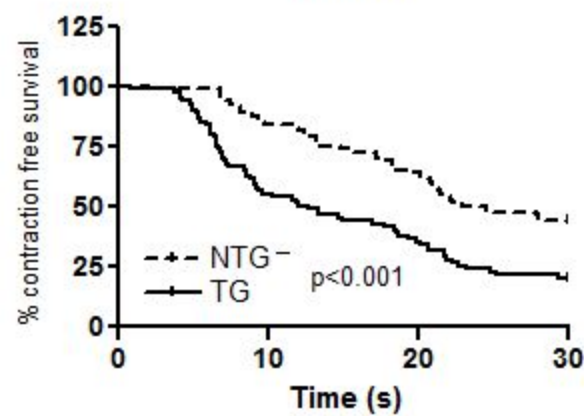
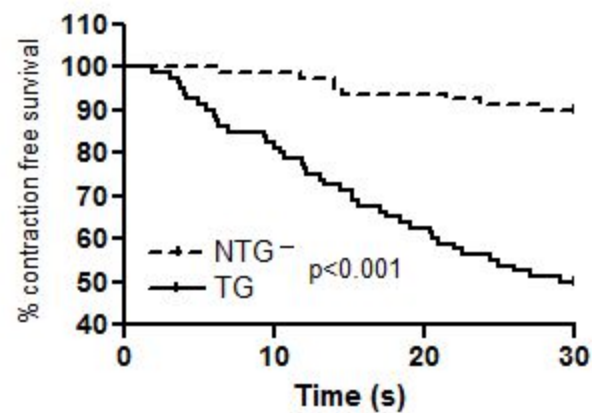


FIG 5





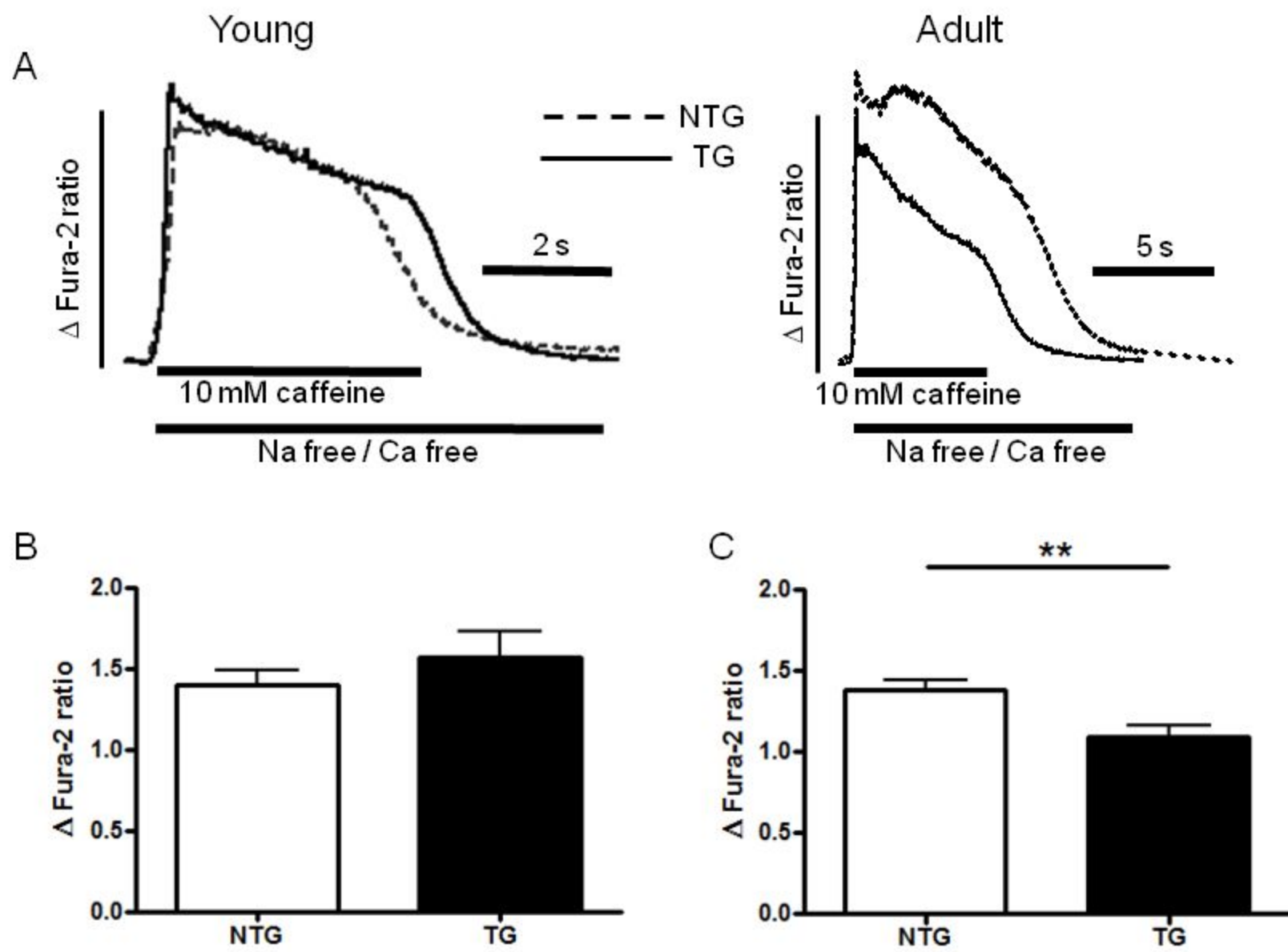
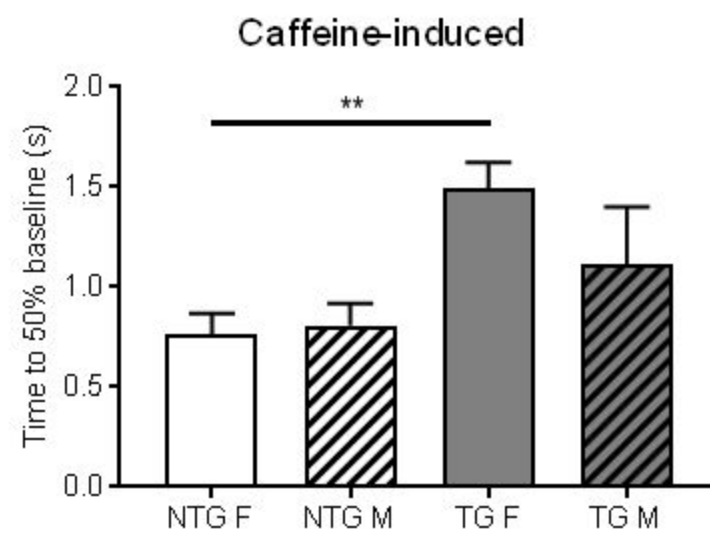
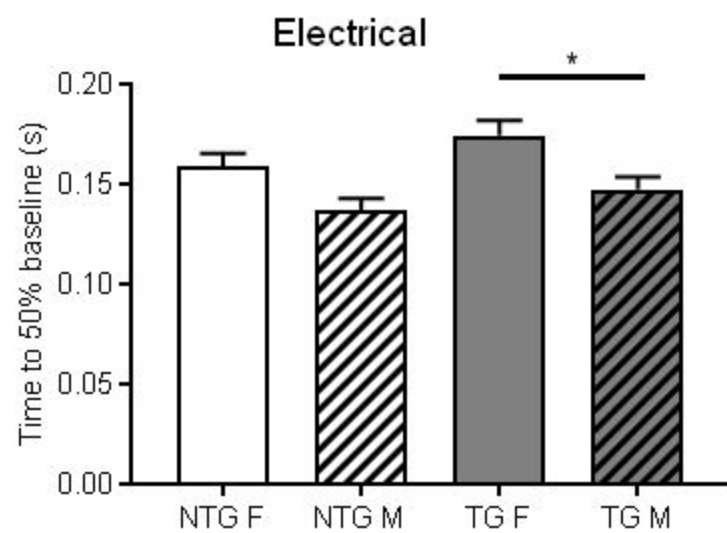


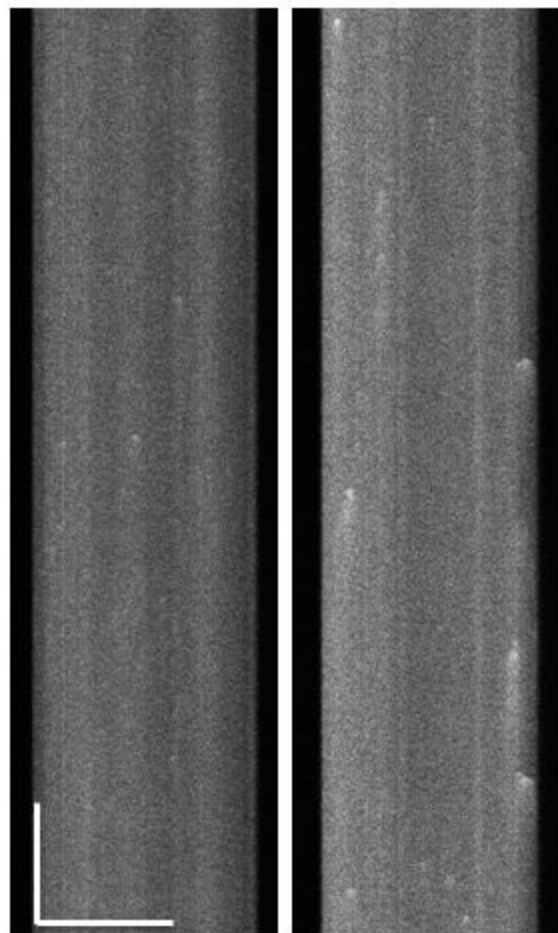
FIG 7



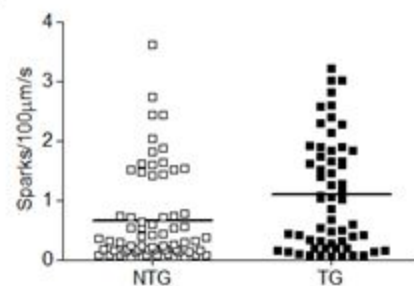
A

NTG

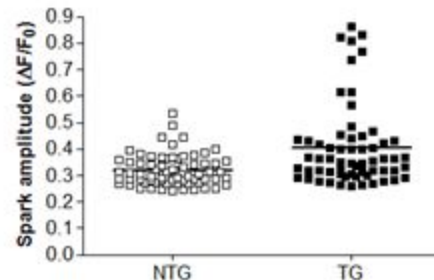
TG



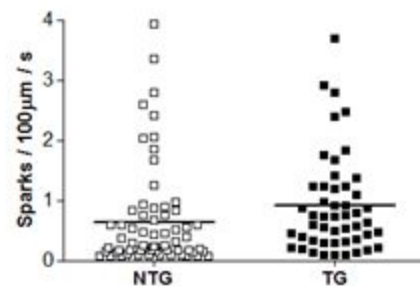
B



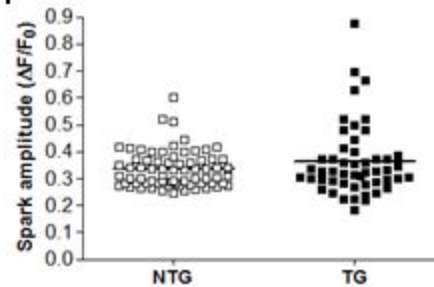
D



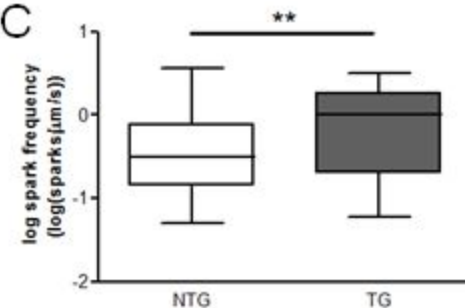
F



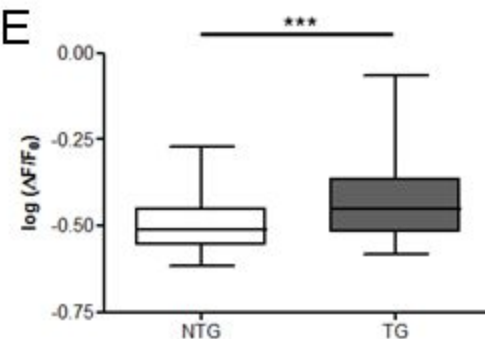
H



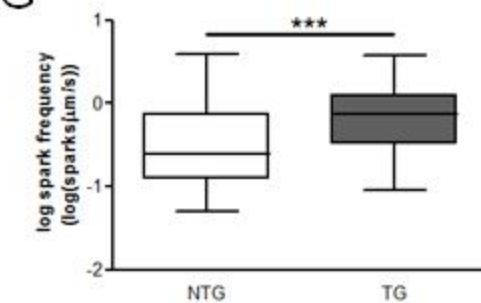
C



E



G



I

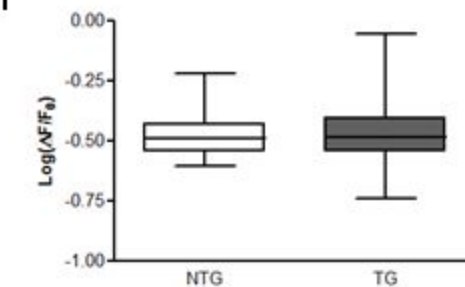


FIG 8

Young

Adult surviving

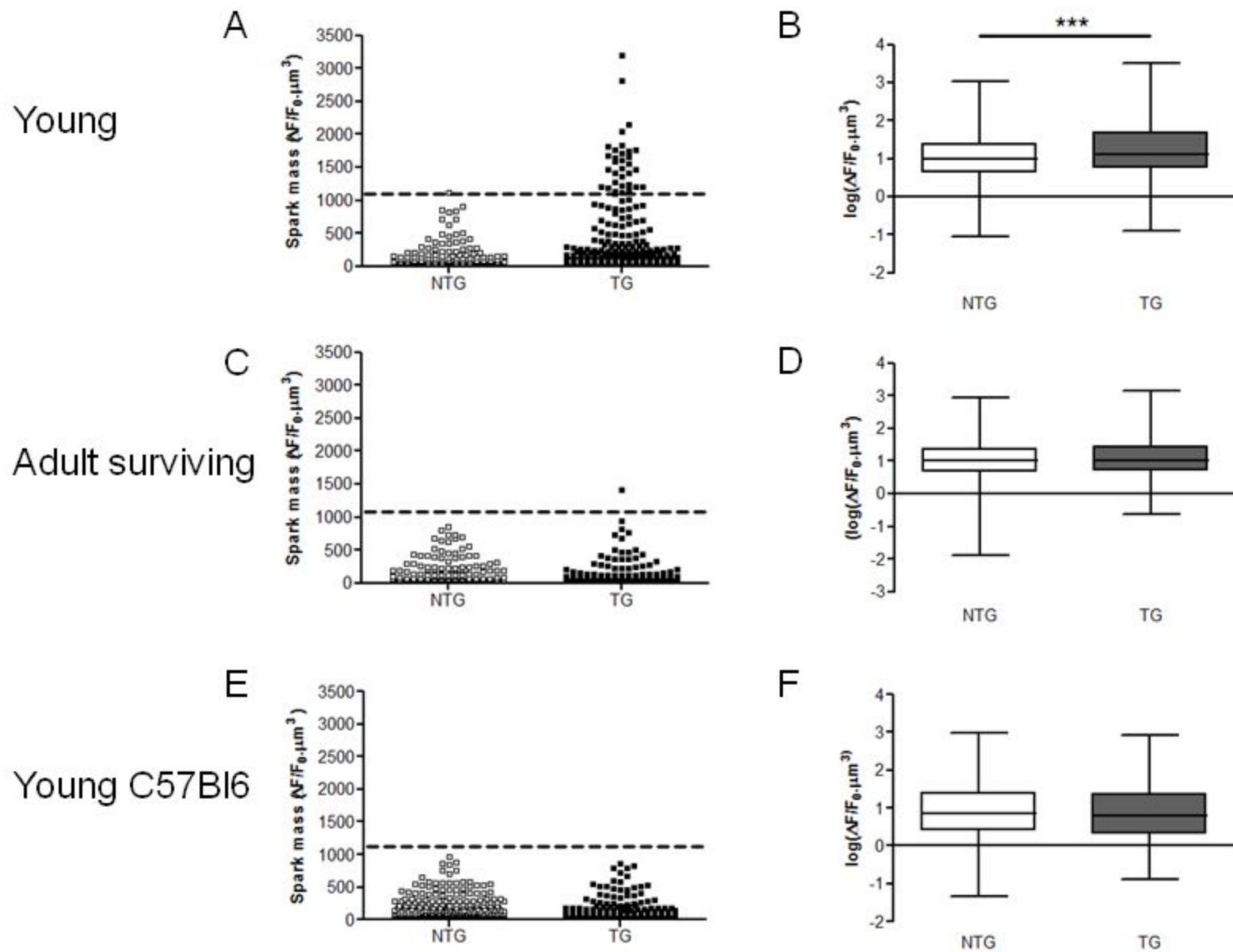


FIG 10

